Investigation of possible fluorophores in human atherosclerotic plaques

Andersson-Engels, Stefan; Gustafson, A; Johansson, Jonas; Stenram, Unne; Svanberg, Katarina; Svanberg, Sune

Published in:
Lasers in Life Science

1992

Lasers in the Life Sciences 5(1–2), 1992, pp. 1–11
Reprints available directly from the publisher
Photocopying permitted by license only

Printed in the United States of America

Investigation of Possible Fluorophores in Human Atherosclerotic Plaque

S. ANDERSSON-ENGELS,[†] A. GUSTAFSON,[‡] J. JOHANSSON,[†] U. STENRAM,[§]
K. SVANBERG,[‡,‖] and S. SVANBERG[†]

[†]Department of Physics, Lund Institute of Technology, P.O. Box 118, S-221 00 Lund, Sweden
[‡]Department of Internal Medicine, Lund University Hospital, S-221 85 Lund, Sweden
[§]Department of Pathology, Lund University Hospital, S-221 85 Lund, Sweden
[‖]Department of Oncology, Lund University Hospital, S-221 85 Lund, Sweden

(Received April 3, 1991; accepted September 17, 1991)

The fluorescence from different depths of atherosclerotically diseased vessels was studied and compared with data for a few purified substances including tryptophan, collagen, elastin, NADH and β-carotene. Both the fluorescence spectra and the fluorescence decay times were used to identify fluorophores in the different layers of plaque. A system consisting of a nitrogen laser (337 nm) and an optical multichannel analyzer connected to the same optical fiber probe was used for the spectral studies. For the fluorescence decay measurements, a mode-locked Ar-ion synchronously pumped dye laser in connection with a photon counting system was used. The dye laser was set at 674 nm to obtain a wavelength of 337 nm after frequency doubling. The fluorescence measurements showed increased fluorescence at 390 nm for atherosclerotic plaque compared with non-diseased vessel wall. This feature was identified as arising from collagen in the tissue. We also found a spectral hump at 520 nm possibly due to carotene in the tissue. The measurements show a substantial distortion of the spectral shape due to the reabsorption of fluorescence by hemoglobin. The extent of the reabsorption was also different for different experimental procedures. The hemoglobin effects were mainly observed when the samples were prepared by mechanical cutting and were not so influential after excimer laser ablation. Methods of eliminating the influence of blood on fluorescence tissue demarcation criteria are discussed.

KEYWORDS: *atherosclerosis, fluorescence, pico-second laser, time-resolved spectroscopy, tissue diagnosis*

INTRODUCTION

Fluorescence spectroscopy as a method for probing different tissue types has developed rapidly during recent years [1–11]. In spite of the lack of sharp features, the spectral shape of the autofluorescence is often sufficient to distinguish between normal and diseased tissue. In such procedures, a thorough knowledge of the fluorescence properties of the possible fluorophores is crucial. Only when such basic research has been done, optimal use of fluorescence in the clinical situation can be expected.

A field in which laser spectroscopy might be of interest as a diagnostic tool is in laser angioplasty in atherosclerotically diseased arteries [12–14]. Early experiments showed occurrence of dissection and perforation of the vessels due to a lack of precise diagnostics. In 1985 it was proposed by Kittrell *et al.* that tissue autofluorescence can be used to character-

ize vessel wall tissue *in vitro* [15]. In the first experiments the blue lines from an argon ion laser were used as an excitation source. Later, it was shown that a significant tissue demarcation could be obtained utilizing UV lasers to excite the tissue fluorescence [16, 17]. Using fluorescence free optical fibers for the UV region, sophisticated multiple fiber probes have been produced for combined diagnostics and treatment. Several criteria for plaque recognition based on tissue fluorescence have been suggested [13, 17, 18]. Both the spectral shape and the fluorescence intensity at a suitable wavelength seem to be relevant for plaque detection. A serious problem with the fluorescence technique was identified recently, namely the strong reabsorption of fluorescence light by hemoglobin which distorts the spectrum [19]. It was shown that many of the features in the fluorescence spectrum are due to the attenuation by blood. In particular, a prominent dip at 420 nm is observed. However, in 1989, we demonstrated two methods for blood independent measurements of tissue fluorescence [20]. In the first one, empirically demonstrated in Ref. 14, two wavelengths are selected, for which the blood attenuation is equal, and where the ratio of the two fluorescence intensities discriminates between plaque and normal tissue. One such pair of wavelengths is 380 nm and 437 nm. A second technique is based on the use of the different fluorescence decay times of diseased and non-diseased vessel wall [14, 21]. Such a recording will be sensitive to the relative occurrence of two fluorophores with different fluorescence decay times, but is independent of a passive light attenuator such as hemoglobin.

Since an atherosclerotic lesion often has a complicated structure with different layers, an important task is to investigate the origin of the different features of the fluorescence spectrum and to identify the fluorophores. Some suggestions can be found in the literature, where carotenoids, vitamin A, tryptophan, etc. are suggested as possible sources of fluorescence [22]. Structures such as collagen and elastin are also probable fluorophores [22, 23].

In this paper we present fluorescence data for various regions of atherosclerotically diseased vessels. Fluorescence spectra were recorded at various depths in the vessel wall, accessed by cutting with a scalpel and by laser ablation with a 308 nm excimer laser. These spectra are compared with fluorescence spectra from tryptophan, β-carotene, nicotinamide adenine dinucleotide (NADH and NAD^+), collagen and elastin. Furthermore, fluorescence decay data, measured with the single-photon counting technique, are presented for the vessel wall layers as well as for the purified substances.

MATERIAL AND METHODS

Fluorescence spectral recordings. As an excitation source a nitrogen laser (Laser Science VSL 337) was used, producing 3 ns pulses of 120 μJ energy at 337.1 nm. The laser light was directed into a 600 μm fluorescence free quartz fiber which was held in contact with the sample. The fluorescence light was collected by the same fiber and directed into an optical multichannel analyzer (EG&G PARC OMA III model 1460) equipped with an image intensified 1024 element diode array detector. Typically 100 shots were recorded to obtain a good signal to noise ratio. The overall spectral resolution of the system was about 10 nm. The system was operated in a region well below photobleaching. The system is described in detail in Ref. 24.

Fluorescence decay time recordings. A mode-locked Ar-ion laser (Coherent Radiation CR

12) was used for synchronous pumping of a dye laser (Coherent Radiation CR 599) to obtain 6 ps pulses at 674 nm. The pulse train was frequency doubled to obtain a wavelength of 337 nm. The excitation spot size was about 0.5 mm in diameter. The fluorescence was captured with a 0.5 m monochromator (Bausch & Lomb) and detected with a microchannel plate photomultiplier (Hamamatsu R 1564 U). The spectral resolution was about 1.5 nm. The trigger signal was obtained with a fast photo diode. The set-up included a time-to-amplitude converter, fast amplifiers, constant fraction discriminators and a multichannel analyzer. The fluorescence decay curves were evaluated in a PC computer using the deconvolution technique to fit up to three lifetime components. The time response function of the apparatus was measured to have a FWHM of 70 ps. A more detailed description is given in Ref. 21.

Samples. Fluorescence data were recorded from aortic samples collected from human autopsies within 24 h *post mortem*. The samples were cleaned of blood and the inner vessel wall was exposed to the laser light. The samples were examined histopathologically for a precise description of the tissue composition. The fluorescence recordings of solutions and powders were performed in a quartz cuvette or an aluminum cup. The substances studied were: L-tryptophan (Sigma Lot 38F-0259) 10 mg/ml in H_2O buffered to pH 7.4, β-NADH (Sigma Lot 639 F6) 0.128 mM in 0.9% saline solution, β-carotene (Sigma type III Lot 78F-0317) 0.1 mg/ml in ethanol, bovine collagen I powder (Sigma Lot 81451) and bovine elastin powder (Sigma Lot 68F-8180). NAD^+, cholesterol and lecithin were also examined but found to exhibit low fluorescence.

RESULTS AND DISCUSSION

The vessels were cut at 45 degrees to the normal of the vessel wall to expose the different layers. Examples of the resulting fluorescence spectra are shown in Figure 1A for the fibrotic layer, yellow lipidic layer, media and adventitia. Some cross-talk between the different layers occurs because of the size of the fiber probe and the finite penetration depth of the laser radiation. In the lower part of the figure the spectrum from mechanically removed lipid rich material in the plaque is shown. When analyzing the spectra in Figure 1 the reabsorption of the fluorescence light by blood must be considered. The absorption profile of hemoglobin is structured and very strong at some wavelengths. To get around the problem of the fluorescence reabsorption, the spectra can be analyzed at pairs of wavelengths with equal blood absorption. Two ratios of such wavelength pairs are 380 nm/437 nm [14] and 520 nm/490 nm. A striking feature of the spectrum from the lipidic substance is the increase in the fluorescence at about 520 nm, most clearly seen in the lower part of Figure 1A. Secondly, the fluorescence at wavelengths shorter than 400 nm is stronger for the fibrotic layer of the plaque. The ratio of the fluorescence at 380 nm and 437 nm is 2.0 for the fibrotic layer and 1.3 for normal vessel wall as well as for the media and adventitia. This is consistent with results reported earlier, e.g. in Ref. 18, where the ratio of the fluorescence at 390 nm to the fluorescence at 480 nm was suggested as a spectroscopic criterion for plaque. For comparison, a spectrum from the surface of a non-diseased vessel wall is given in Fig. 1B. It is interesting to note the similarity of the normal vessel wall and the deeper non-affected layers of the plaque over the whole range of the spectrum.

The important features of Figure 1A are shown in Figure 2 in scans from the vessel wall surface of a plaque to the adventitia for seven different samples. The crosses indicate the

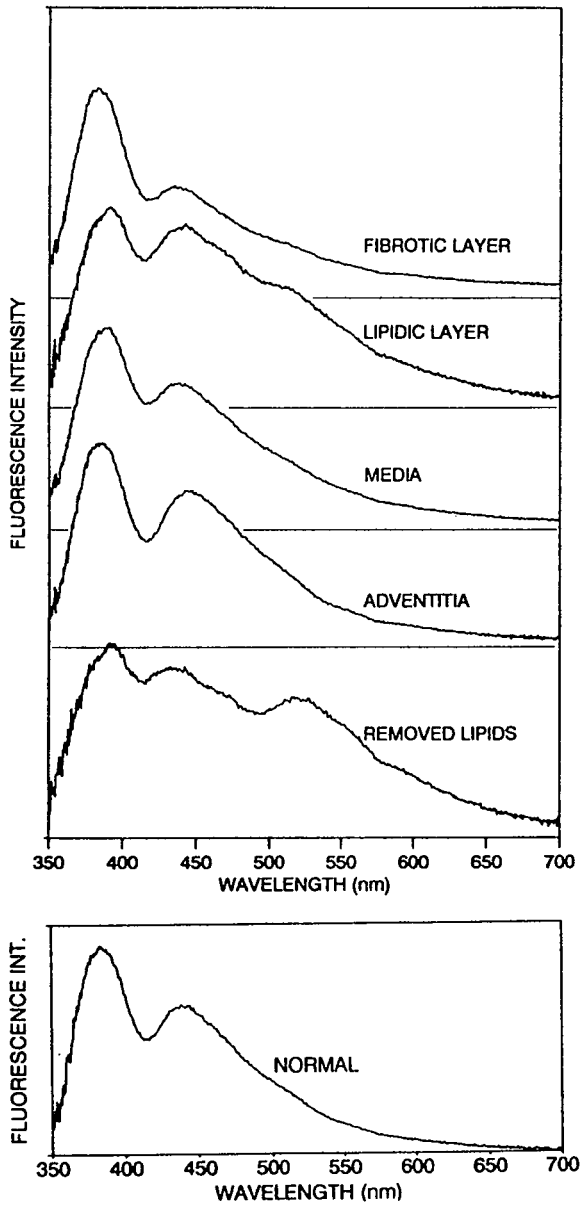

FIGURE 1 A: Fluorescence spectra from different layers of an atherosclerotically diseased vessel wall using nitrogen laser excitation (337 nm). The samples are from top to bottom: fibrotic layer, lipid-rich yellow layer, non-diseased media, adventitia and lipid-rich yellow substance removed from the plaque. B: Fluorescence spectrum from the surface of a non-diseased piece of an aortic vessel wall. The excitation wavelength was 337 nm.

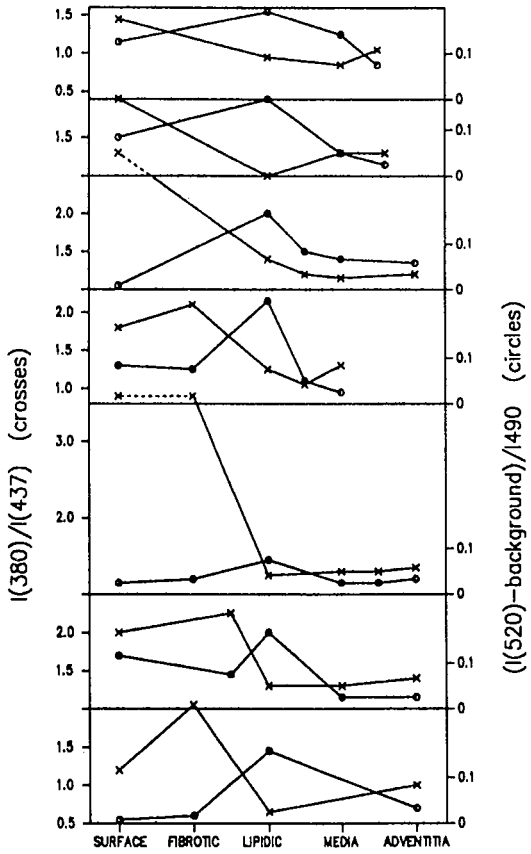

FIGURE 2 Scans through seven different regions, from fibrotic tissue to non-diseased media and adventitia. Crosses indicate I(380 nm)/I(437 nm) (left scale) while circles indicate (I(520 nm) − background)/I(490 mn) (right scale). The fluorescence background at 520 nm was calculated using an exponential fit between 485 nm and 650 nm excluding the peak.

ratio of the fluorescence intensities at 380 nm and 437 nm, while the circles indicate the ratio of the fluorescence intensities at 520 nm and 490 nm where the 520 nm peak is lifted off the slope of the fluorescence spectrum. Here we clearly see the large amount of the 520 nm fluorophore in the lipidic region. We also observe a high value for the 380 nm/437 nm ratio for the surface and the fibrotic layers.

The next experiment was performed using a 308 nm excimer laser (100 mJ/pulse, 10 ns, spot size about 0.5 mm) to ablate the plaque samples. Fluorescence spectra were recorded for various depths of the ablation crater corresponding to different numbers of excimer laser shots. The fluorescence spectra, obtained with a nitrogen laser, are shown in Figure 3 for a typical series of 0, 10, 20, 40 and 80 excimer laser shots, again as a plaque depth scan. The insert in Figure 3 shows an example of an ablation crater. When comparing Figure 1A and Figure 3, a strong similarity between the two scans for the upper fibrotic layer can be observed. However, for the deeper layers, the absence of a spectral dip at 420 nm, which is due to absorption by hemoglobin, is noted. The reason for this may be a bleaching of the

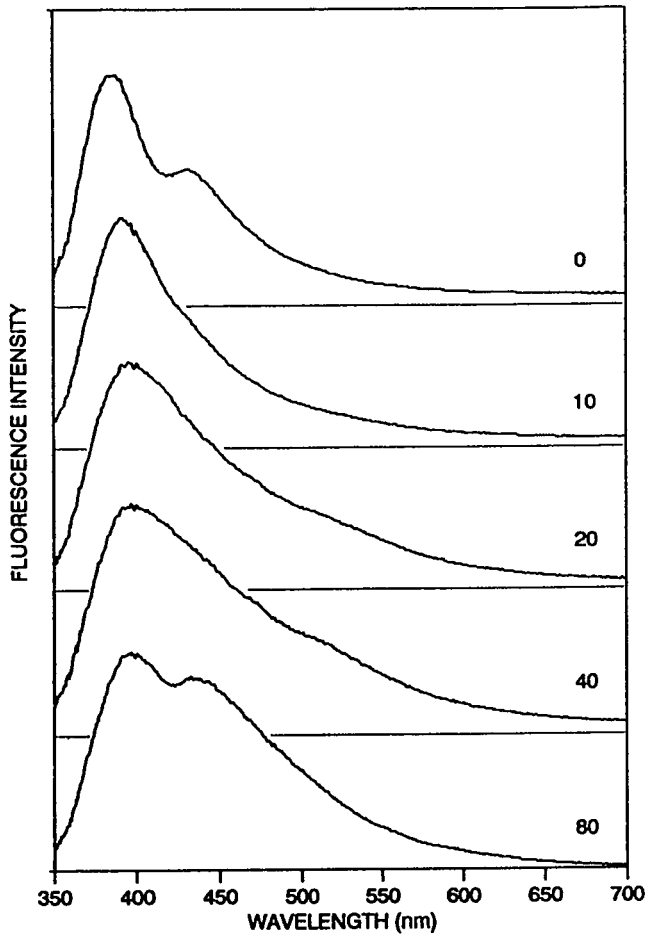

FIGURE 3 Fluorescence spectra of a plaque region for various ablation crater depths. The fluorescence excitation wavelength was 337 nm and all spectra are normalized. For ablation an excimer laser (308 nm, 100 mJ) was used. A histological cut of an ablation crater of a depth of 1.5 mm is inserted. From top to bottom, 0, 10, 20, 40 and 80 excimer pulses were applied. The corresponding craters extended over: surface, fibrotic plaque, fibrotic/lipidic plaque, lipidic plaque and lastly lipidic plaque/media.

hemoglobin molecules. Whatever the reason for this absence of blood interference in the fluorescence spectra, it is a feature of importance for fluorescence guided *in vivo* laser ablation of plaque. It was earlier pointed out by us that a spectroscopic plaque criterion must be insensitive to the presence of blood for a reliable diagnosis during laser angioplasty. This will be true also in this case since the degree of bleaching of the hemoglobin molecules is dependent on the laser ablation.

Examples of the fluorescence recordings of the purified substances using nitrogen laser excitation are shown in Figure 4. The samples are, from left to right: tryptophan, collagen I, elastin, NADH and β-carotene. It should be pointed out that the curves are not presented on the same scale, and must be compared only on the basis of spectral shape. However, it is

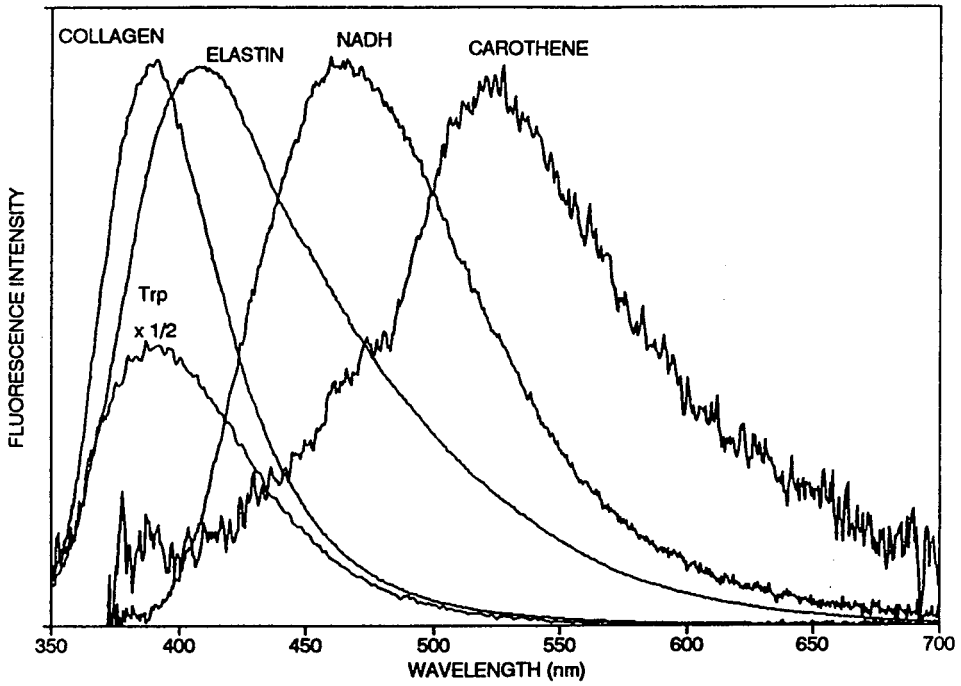

FIGURE 4 Fluorescence spectra from tryptophan, collagen I, elastin, NADH and β-carotene using nitrogen laser excitation (337 nm).

worth mentioning that the fluorescence for tryptophan and β-carotene solutions seems to be substantially weaker than that for the other substances at the concentrations and excitation wavelength used. In Figure 1A, a fluorescence peak at 520 nm was observed mainly in the lipidic part of the plaque. It is possible that the peak at 520 nm is caused by β-carotene, shown in Figure 4. One should be careful with conclusions in this spectral region where hemoglobin has two absorption maxima at 540 nm and 580 nm, but in this case we can also see a small trace of these as dips in the spectrum from removed lipids in Figure 1A. Thus it is likely that the 520 nm peak is a true fluorescence contribution to the spectrum. Another point about β-carotene is the possibility of impurities in the solution, which might be fluorescent in the wavelength region. Also, in Ref. 11 ceroids are suggested as a possible source of fluorescence in lipidic plaques.

For the fibrotic part of the plaque in Figure 1A, we observed strong fluorescence at about 390 nm. This correlates well with the collagen spectrum in Figure 3. It was recently suggested that a main feature of the spectral differences between plaque and normal vessel tissue is due to the relative proportions of collagen and elastin [17]. The scans shown in Figure 1A and Figure 3 give support to this theory as the fluorescence seems to shift towards longer wavelengths when going deeper into the plaque, approaching non-diseased tissue. This can be expressed in terms of blood independent data. It can be seen in Figure 4 that the broader fluorescence spectrum of elastin peaks at a longer wavelength than collagen. The ratio I(380 nm)/I(437 nm) is about 3 for collagen but only 0.8 for elastin. The same ratio was for fibrotic plaque 2.0 and for normal 1.3. When going even further into the vessel wall,

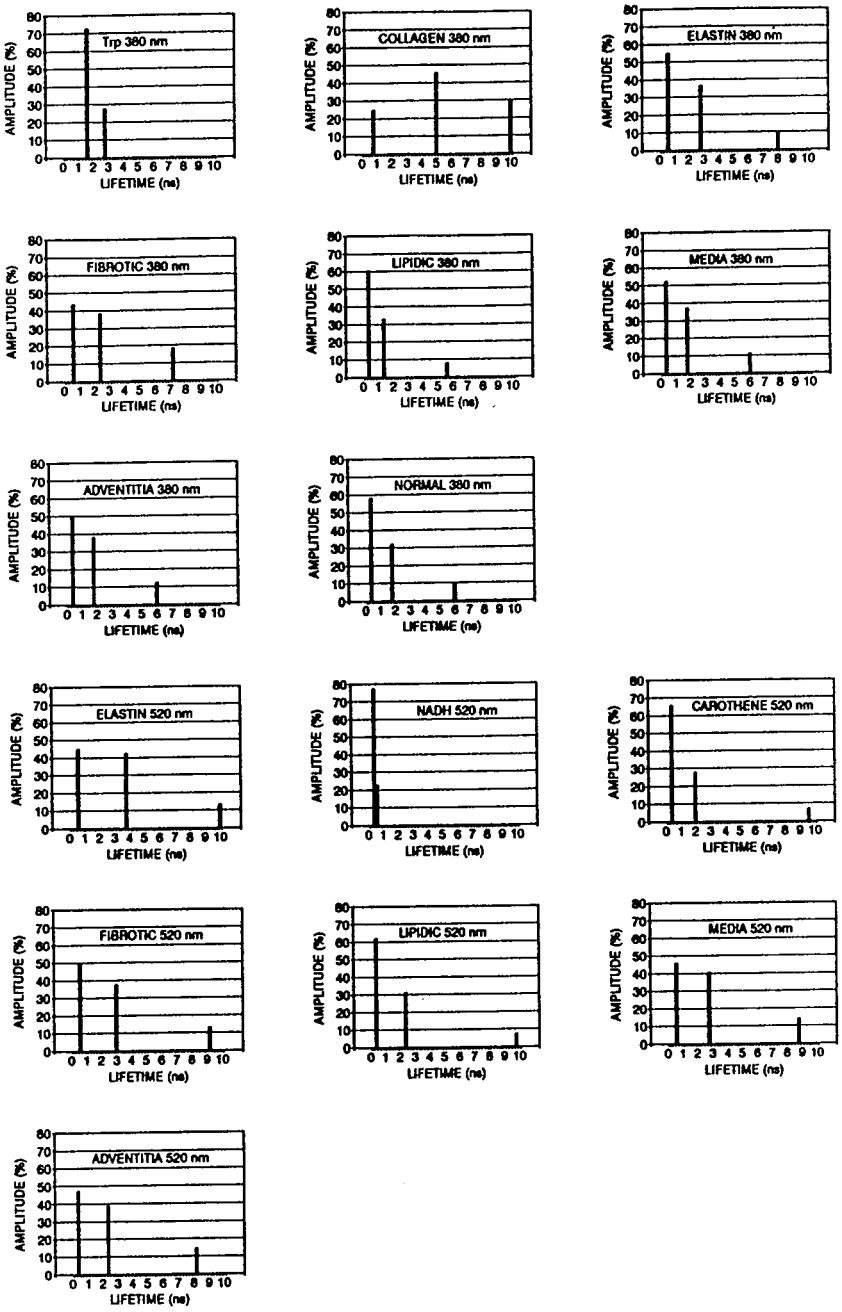

FIGURE 5 Fluorescence decay data for tryptophan, collagen I, elastin, NADH, β-carotene, different plaque layers and normal vessel wall plotted as the fluorescence decay amplitudes as a function of fluorescence decay times. The excitation source was a mode-locked Ar-ion laser pumped dye laser, frequency doubled to 337 nm. The fluorescence was detected at 380 nm and 520 nm. The decay curves were fitted to a multi-exponential decay: $I(t) = \sum_K A_k \cdot \exp(-t/\tau_k)$.

entering the non-diseased media and adventitia, the spectral shape shifts further to the red. Thus, it is likely that some other fluorophore is involved in this vessel region. The media and adventitia are well vascularized tissue with the network of the supplying vessels, *vasa vasorum*. We have suggested that the main fluorophore in muscle tissue might be nicotinamide adenine dinucleotide (NADH), [25] a strongly fluorescing chromophore peaking at 470 nm, [26, 27] also seen in Figure 4. It is possible that the strong fluorescence from NADH can be observed in the adventitia.

It is obvious that the identification of tissue fluorophores based solely on the shape of the fluorescence spectrum is ambiguous and uncertain, since two different fluorophores may give rise to the same spectrum. However, if the fluorescence decay time properties are included in the analysis, the probability of an adequate identification increases. In Figure 5 the fluorescence decay times and corresponding amplitudes are plotted for the same purified fluorophores as presented in Figure 4. The decay data for the different plaque layers shown in Figure 1 are also plotted in Figure 5. When studying Figure 5 it is important to remember that the time integrated fluorescence at a certain wavelength is proportional to $A \cdot \tau$ for each decay component. Thus, the slower decay components are important in spite of the low amplitudes. Firstly, it can be seen in Figure 5 that the fluorescence decay at 380 nm for collagen is slower than for elastin. Secondly, the slow decay component for the fibrotic plaque layer is about twice as high as for the other plaque layers and normal vessel wall. A comparison of the decay data for collagen, elastin, normal and plaque layers therefore gives further support to the theory that collagen and elastin are the main fluorescing tissue components in the artery wall, with a higher relative proportion of collagen in fibrotic plaque. From Figure 4 one is tempted to believe that tryptophan might be a main fluorophore in fibrotic plaque tissue. However, the different decay properties suggest that this is not the case. The lipidic part of the plaque seems to contain less of the long-lived fluorescence component. This could partly be due to β-carotene. The decay time for NADH is, in comparison with the other substances in Figure 5, much shorter. If NADH can be found in the deeper layer of the plaque as speculated above, it would be easy to see this using 337 nm excitation. However, we cannot see any such short fluorescence decay time when entering the adventitia. Therefore, it is not likely that the fluorescence observed from the adventitia layer originates from NADH. A better guess would probably be that the major fluorophore in this region is elastin, judged from Figure 5.

From Figure 5 it is clear that collagen has a much more intense long-lived fluorescence component than elastin. This reflects the pattern observed for atherosclerotic plaque in comparison with non-diseased vessel wall. We have also found that collagen has its fluorescence peak at 390 nm, whereas for elastin it is found at about 410 nm, also showing a much broader spectrum. Again, this is in agreement with what we see for plaque and normal vessel wall, respectively. Thus, the most probable interpretation of these findings is that the spectroscopic difference in the 390 nm region between plaque and normal vessel is due to a change in the relative occurrence of collagen and elastin in the tissue.

Acknowledgments

This work was supported by the Swedish Cancer Society, the Swedish Council for Medical Research, the Knut and Alice Wallenberg Foundation and the Swedish Board for Technical Development.

References

1. van Hoek, A., Vos, K., and Visser, A.: Ultrasensitive time-resolved polarized fluorescence spectroscopy as a tool in biology and medicine, *IEEE J. Quant. Electron.* **QE-23**, 1812–1820, 1987.
2. Letokhov, V. S.: *Laser Picosecond Spectroscopy and Photochemistry of Biomolecules*, Adam Hilger, Bristol, Philadelphia, 1987.
3. Rigler, R., Claesens, F., and Kristensen, O.: Picosecond fluorescence spectroscopy in the analysis of structure and motion of biopolymers, *Anal. Instr.* **14**, 525–546, 1985.
4. Meech, S. R., Stubbs, C. D., and Phillips, D.: The application of fluorescence decay measurements in studies of biological systems, *IEEE J. Quant. Electron.* **QE-20**, 1343–1352, 1984.
5. Profio, A. E., Doiron, D. R., Balchum, O. J., and Huth, G. C.: Fluorescence bronchoscopy for localization of carcinoma in situ, *Med. Phys.* **10**, 35–39, 1983.
6. Andersson-Engels, S., Ankerst, J., Johansson, J., Svanberg, K., and Svanberg, S.: Tumour marking properties of different haematoporphyrins and tetrasulfonated phthalocyanine—a comparison, *Lasers Med. Sci.* **4**, 115–123, 1989.
7. Yang, Y., Ye, Y., Li, F. Li, Y., and Ma, B.: Characteristic autofluorescence for cancer diagnosis and its origin, *Lasers Surg. Med.* **7**, 528, 1987.
8. Alfano, R. R., Tata, D. B., Cordero, J., Tomashefsky, P., Longo, F. W., and Alfano, M. A.: Laser-induced fluorescence spectroscopy from native cancerous and normal tissue, *IEEE J. Quant. Electron.* **QE-20**, 1507–1511, 1984.
9. Andersson-Engels, S., Johansson, J., and Svanberg, S.: Multicolor fluorescence imaging system for tissue diagnostics, *Proc. SPIE* **1205**, contr. 19, 1990.
10. Andersson-Engels, S., Johansson, J., Svanberg, K., and Svanberg, S.: Fluorescence diagnostics and photochemical treatment of diseased tissue using lasers, *Anal. Chem.* part I: **61**, 1367–1373, 1989, Part II: **62**, 19–27, 1990.
11. Fitzmaurice, M., Bordagaray, J. O., Engelmann, G. L., Richards-Kortum, R., Kolubayev, T., Feld, M. S., Ratliff, N. B., and Kramer, J. R.: Argon ion laser-excited auto fluorescence in normal and atherosclerotic aorta and coronary arteries: Morphologic studies. *Am. Heart J.* **118**, 1029–1038, 1989.
12. Prince, M. R., Deutsch, T. F., Mathews-Roth, M. M., Margolis, R., Parrish, J. A., and Osteroff, A. R.: Preferential light absorption in atheromas in vitro, *J. Clin. Invest.* **78**, 295–302, 1986.
13. Cothren, R. M., Hayes, G. B., Kramer, J. R., Sachs, B., Kittrell, C., and Feld, M. S.: A multifiber catheter with an optical shield for laser angiosurgery, *Lasers Life Sci.* **1**, 1–12, 1986.
14. Andersson-Engels, S., Johansson, J., Stenram, U., Svanberg, K., and Svanberg, S.: Malignant tumor and atherosclerotic plaque diagnostics using laser-induced fluorescence, *IEEE J. Quant. Electron.* **26**, 2207–2217, 1991.
15. Kittrell, C., Willett, R. L., de los Santos Pacheo, C., Ratliff, N. B., Kramer, J. R., Malk, E. G., and Feld, M. S.: Diagnosis of fibrous arterial atherosclerosis using fluorescence, *Appl. Opt.* **24**, 2280–2281, 1985.
16. Andersson, P. S., Gustafson, A., Stenram, U., Svanberg, K., and Svanberg, S.: Diagnosis of arterial atherosclerosis using laser-induced fluorescence, *Lasers Med. Sci.* **2**, 261–266, 1987.
17. Laifer, L. I., O'Brien, K. M., Stetz, M. L., Gindi, G. R., Garrand, T. J., and Deckelbaum, L. I.: Biochemical basis for the difference between normal and atherosclerotic arterial fluorescence, *Circulation* **80**, 1893–1901, 1989.
18. Andersson-Engels, S., Gustafsson, A., Johansson, J., Stenram, U., Svanberg, K., and Svanberg, S.: Laser-induced fluorescence used in localizing atherosclerotic lesions, *Lasers Med. Sci.* **4**, 171–181, 1989.
19. Oraevsky, A. S., Letokhov, V. S., Ragimov, S. E., Omelyanenko, V. G., Belyaev, A. A., Shekhonin, B. V., and Akchurin, R. S.: Spectral properties of human atherosclerotic blood vessel wall, *Lasers Life Sci.* **2**, 275–288, 1988.
20. Andersson-Engels, S., Johansson, J., Stenram, U., Svanberg, K., and Svanberg, S.: Time-resolved laser-induced fluorescence spectroscopy for enhanced demarcation of human atherosclerotic plaques, *J. Photchem. Photobiol.* **4**, 363–369, 1990.
21. Andersson-Engels, S., Johansson, J., and Svanberg, S.: The use of time-resolved fluorescence for diagnosis of atherosclerotic plaque and malignant tumours. *Spectrochim. Acta* **46A**, 1203–1210, 1990.
22. Leon, M. B., Lu, D. Y., Prevosti, L. G., Macy, W. W., Smith, P.D., Granovsky, M., Bonner, R. F., and Balaban, R. S.: Human arterial surface fluorescence: Atherosclerotic plaque identification and effects of laser atheroma ablation, *J. Am. Coll. Cardiol.* **12**, 94–105, 1988.
23. Baraga, J. J., Taroni, P., Park, Y. D., An, K., Maestri, A., Tong, L. L., Rava, R. P., Kittrell, C., Dasari, R. R., and Feld, M. S.: Ultraviolet laser induced fluorescence of human aorta, *Spectrochim. Acta* **45A**, 95–99, 1989.
24. Andersson-Engels, S., Elner, Å., Johansson, J., Karlsson, S-E., Salford, L., Strömblad, L-G., Svanberg, K., and Svanberg, S.: Clinical recordings of laser-induced fluorescence spectra for evaluation of tumour demarcation feasibility in selected clinical specialties, *Laser Med. Sci.* In press.

25. Andersson-Engels, S., Johansson, J., Svanberg, K., and Svanberg, S.: Fluorescence imaging and point measurements of tissue: applications to the demarcation of malignant tumors and atherosclerotic lesions from normal tissue, *Photochem. Photobiol.* **53**, 807–814, 1990.
26. Lohman, W., Mussman, J., Lohman, C., and Kûnzel, W.: Native fluorescence of the cervix uteri as a marker for dysplasia and invasive carcinoma, *Eur. J. Obstet. Gynecol. Reprod. Biol.* **31**, 249–253, 1989.
27. Lohman, W. and Paul, E.: Native fluorescence of unstained cryosections of the skin with melanomas and naevi, *Naturwissenshaften* **76**, 424–426, 1989.